On the Stability of a Detailed Packed-Bed Reactor

M. L. MC GUIRE and LEON LAPIDUS

Princeton University, Princeton, New Jersey

An analysis of the stability of a packed-bed reactor is presented subject to a model including axial and radial gradients in the interparticle field and gradients plus reaction in the intraparticle field. The stability of the entire reactor is characterized in terms of various stable and unstable conditions inside the porous particles. Simplifications in the mathematical model are shown to be invalid in many situations.

The recent availability of large scale digital computers has led to an increased interest in the mathematical representation and simulation of packed-bed reactors. This representation is extremely complicated since gradients in the external field exist in many directions and must be considered simultaneously with the heat and mass transport inside the particles. Even when the steady state system alone is considered, a complex set of differential equations arises, and with the further addition of the dimension of time, the problem becomes even more difficult to solve.

Of primary concern in defining the operation of a packed-bed catalytic reactor is the need to specify the stability of such reactors. Stability is here taken to mean that the reactor does not run away when the feed conditions are subject to perturbations in temperature or mass. However, it is necessary to know the transient response of a reactor in order to reach some valid quantitative conclusions regarding the stability.

In the present work a mathematical model is presented for describing the transient behavior of a packed-bed catalytic reactor. This model includes many of the important mechanisms necessary to an accurate description of the transport phenomena occurring in such reactors. The model is then simulated on a digital computer, the IBM-7090, to ascertain the effect of feed perturbations on the transient response of the reactor. Of primary concern in the results obtained is the fact that the use of simplifying assumptions to remove some of the complexity in the model can lead to misleading results. On this basis it may well be that the only procedure for obtaining valid packed-bed reactor profiles is to use a model of the profundity presented here. In addition, stability is seen to be connected directly to the behavior of the internal particles, more so than to the external field.

BACKGROUND INFORMATION

The literature dealing with the description and simulation of packed-bed reactors is voluminous. The recent works of Beek (*4*) and Wilhelm (*18*) outline in detail many of the facets of the work carried out to date. Rather than repeat much of these descriptions, only a brief outline of certain of the previous literature will be discussed here. This will serve to place a proper perspective on the work and results to be discussed.

The stability of chemical reactors has been studied for a number of years. Thus van Heerden (*15*) and Aris and Amundson (*1*) concentrated on the continuous-stirred-tank-reactor (CSTR), and by using linearized heat and mass balances and treating the resultant set of equations by the methods of classical linear mechanics they came up with a generally valid stability criterion for this particular system. However, even in the simplified case of the packed-bed reactor (with internal particle gradients neglected), the dependent variables are functions of three independent variables: distance in the axial direction, distance in the radial direction, and time. On this basis the transient behavior can be described only by sets of partial differential equations. Unfortunately the boundary-value nature of this system and the type of system itself precludes anything beyond the beginnings of classical analysis. Thus the only resort to obtaining transient profiles is simulation by a computer.

Recently Deans and Lapidus (*7*) have shown how this partial differential equation model may be converted into an equivalent initial value problem involving a selected array of CSTR's. On this basis the calculation of the transient response of fixed-bed reactors begins to approach feasibility. However even in this case there may be some computational problems (*8*). This is further accented when the model is extended to include chemical reaction inside the catalyst particles instead of assuming an external surface reaction mechanism. However, Carberry and Wendel (*6*) have simulated the behavior of beds of porous solids with particular emphasis on selectivity in the steady state.

The detailed treatment of the stability of fixed-bed reactors was initiated by such authors as Barkelew (*2*) and Liu and Amundson (*11*). However, in each case simplifying assumptions were made in order to be able to carry out the analysis. Barkelew neglected axial and radial gradients as well as internal particle gradients and cast the resulting system into a steady state form. Liu and Amundson included the axial gradients and solved the resulting partial differential equations. In both of these cases, even with the simplifying assumptions made, computer solutions were required.

When one considers the assumptions required in these and other analyses of this type, it seems apparent that the results may be subject to considerable error especially when applied to beds which are made up of porous particles and in which extensive chemical reaction is occurring.

THE TRANSIENT BEHAVIOR OF A SINGLE CATALYST PARTICLE

Since a major factor neglected in previous fixed-bed reactor analyses is the contribution due to catalyst particles which are porous and large enough for the diffusion and reaction mechanisms to be competitive, it is instructive to first consider this factor by itself. It is important to note that in the last three years a number of authors,

M. L. McGuire is with the School of Chemical Engineering and Materials Science, University of Oklahoma, Norman, Oklahoma.

Schillson and Amundson (*14*), Carberry (*5*), Weisz and Hicks (*17*), and others, have theoretically discovered the existence of multiple steady states or equilibrium conditions for selected values of the physical parameters of a single catalytic particle.

Steady State System

Consider a single catalyst particle which is bathed in an infinite fluid. On the assumption that the particle is large enough to permit mass and temperature gradients inside the particle, the steady state mass and heat balances within the particle are given by

$$D_p \nabla^2 c' + N_R = 0 \tag{1}$$

$$k \nabla^2 T' + \Delta H N_R = 0 \tag{2}$$

For a first-order reaction with the familiar Arrhenius reaction rate expression, the rate expression can be explicitly written as

$$N_R = -k' c' = -a c' e^{-E/R_1 T'}$$

where N_R is rate of appearance, or with $k_o = a e^{-E/R_1 T_o}$ and $\Delta T = T' - T_o$, where T_o is the surface temperature, as

$$N_R = -k_o c' \exp\left\{\frac{E}{R_1 T_o}\left[\frac{\Delta T}{T_o}\left(\frac{1}{1+\Delta T/T_o}\right)\right]\right\} \tag{3}$$

Prater (*13*) has shown that for any particle geometry the temperature at any point inside the particle can be related to the surface temperature and composition by

$$\Delta T = T' - T_o = -\frac{\Delta H D_p}{k}(c_o - c') \tag{4}$$

Using this relationship in Equation (3) one can write the rate expression in terms of a single variable as follows:

$$N_R = -k_o c' \exp\left\{\frac{E}{R_1 T_o}\left[\frac{-\Delta H D_p (c_o - c')}{k T_o}\,\frac{1}{1+\left[\frac{-\Delta H D_p}{k T_o}(c_o - c')\right]}\right]\right\} \tag{5}$$

Finally, the definition of the dimensionless variables

$$\begin{aligned} c &= c'/c_o \\ \rho &= r/R \\ \gamma &= E/R_1 T_o \\ \beta &= \frac{c_o \Delta H D_p}{k T_o} \\ \delta &= \frac{R^2 k_o}{D_p} \end{aligned} \tag{6}$$

and the substitution of Equation (5) into the spherical coordinate form of Equation (1) yields

$$\frac{d^2 c}{d\rho^2} + \frac{2}{\rho}\frac{dc}{d\rho} = \delta c \exp\left[\frac{-\gamma\beta(1-c)}{1-\beta(1-c)}\right] \tag{7}$$

When this equation is integrated, it yields the steady state concentration profile within the particle; the corresponding temperature profile follows from the dimensionless equivalent of Equation (4).

Of interest here is that if the parameters $\gamma = 20.0$, $\beta = -0.6$ (an exothermic reaction), and $\delta = 0.25$ are chosen, the numerical solution of Equation (7) yields three possible composition profiles: one corresponding to high reaction, the second corresponding to low reaction, and the third corresponding to an intermediate degree of reaction. These results, while not shown here, will be used shortly. Such multiple solutions are, of course, more unusual in actual practice than the single solution system since they result from a careful and narrow selection of the system parameters (*17*). However, in order to analyze the behavior of the current model under a comparatively complicated situation, it was decided to use the multiple solution system.

Transient System

The transient heat and mass balances for the single catalyst particle are similar to the steady state system except for the addition of an accumulation term. Explicitly these balances are

$$\rho_s c_s \frac{\partial T'}{\partial t'} = k \nabla^2 T' + \Delta H N_R \tag{8}$$

$$\alpha \frac{\partial c'}{\partial t'} = D_p \nabla^2 c' + N_R \tag{9}$$

The balances for the film at the particle surface are given by

$$\frac{\partial c'(S)}{\partial r} = \frac{k_g}{D_p}[c_f' - c'(S)], \quad r = R \tag{10}$$

$$\frac{\partial T'(S)}{\partial r} = \frac{h_f}{k}[T_f' - T'(S)], \quad r = R \tag{11}$$

These equations may be cast into a dimensionless form by defining

$$T = T'/T_o \qquad \rho = r/R$$
$$c = c'/c_o \qquad t = t'v/d_p$$

and the dimensionless groups

$$N_1 = \frac{d_p v \rho_s c_s}{k}$$

$$N_2 = \frac{d_p v}{D_p}$$

$$\text{Modified Nusselt number} = N'_{Nu} = \frac{h_f d_p}{k}$$

$$\text{Modified Sherwood number} = N'_{Sh} = \frac{k_g d_p}{D_p}$$

Equations (8) to (11) now become

$$\frac{N_1}{4}\frac{\partial T}{\partial t} = \frac{\partial^2 T}{\partial \rho^2} + \frac{2}{\rho}\frac{\partial T}{\partial \rho} - \delta \beta c e^{-\gamma\left[\frac{1}{T}-1\right]} \tag{12}$$

$$\alpha\frac{N_2}{4}\frac{\partial c}{\partial t} = \frac{\partial^2 c}{\partial \rho^2} + \frac{2}{\rho}\frac{\partial c}{\partial \rho} - \delta c e^{-\gamma\left[\frac{1}{T}-1\right]} \tag{13}$$

$$\frac{\partial c(S)}{\partial \rho} = \frac{N'_{Sh}}{2}[c_f - c(S)], \quad \rho = 1.0 \tag{14}$$

$$\frac{\partial T(S)}{\partial \rho} = \frac{N'_{Nu}}{2}[T_f - T(S)], \quad \rho = 1.0 \tag{15}$$

In order to uniquely determine the system of equations, a set of boundary conditions must be specified, and a consistent set of these is given as

$$\frac{\partial T}{\partial \rho} = \frac{\partial c}{\partial \rho} = 0, \quad \rho = 0 \tag{16}$$

$$T_{\text{fluid}} = T_f(t) \tag{17}$$

$$c_{\text{fluid}} = c_f(t) \tag{18}$$

Details of the numerical treatment of these equations are given in a later section of this paper.

A number of transient computations were carried out

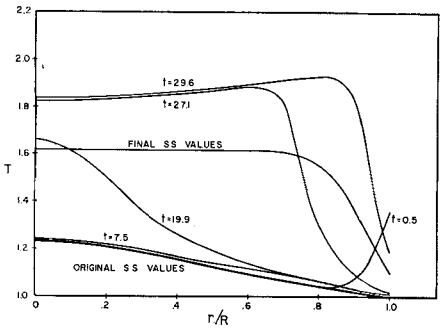

Fig. 1. Particle temperature profiles at various times after a positive temperature perturbation, $\beta = -0.6$, $\gamma = 20$, $\delta = 0.25$.

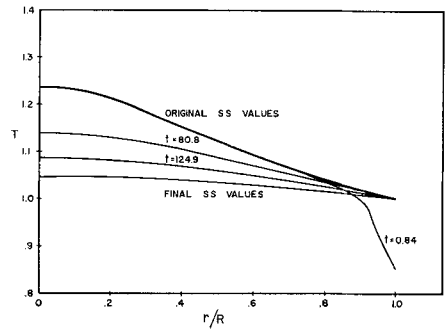

Fig. 2. Particle temperature profiles at various times after a negative temperature perturbation.

with the steady state equations of the system to generate an initial mass and temperature profile. With the particle at this steady state, a pulse perturbation in temperature of short duration was applied. The transient response to this perturbation was observed until steady state was reached.

The choice of the initial profile is very important since the middle or intermediate steady state is unstable to any size perturbation while the other two states are stable. However, stable here is defined with respect to a small perturbation since large perturbations (10 to 15% increase or decrease in surface temperature) are sufficient to move the system from the upper steady state to the lower and vice versa.

Figure 1 shows the transient response of the particle temperature to a positive pulse perturbation in temperature with the initial profile being the intermediate steady state. As can be seen, there is an initial temperature rise near the particle surface; this is followed by a temperature wave towards the center line of the particle. However, as the temperature rises at the center, it in turn starts another temperature wave towards the particle surface. The eventual steady state values, corresponding to the high reaction profile, are about 20 to 30% lower than the maximum temperature rise.

This rather straightforward example shows very definitely that the consideration of only steady state profiles can be very misleading. The response to the perturbation is very slow at first owing to the essentially linear conduction mechanism, but when the temperature gets high enough, the reaction becomes very fast and perhaps even approaches a runaway. If the upper physical temperature limit of the pellet is not too far above the final steady state value, then it is apparent that the pellet response will be unstable even though the steady state values do not indicate same.

In Figure 2 the same initial steady state profile is used for the transient calculation, but in this case the temperature perturbation is negative. As is evident, the behavior is completely different from that of Figure 1, with a gradual approach to the lower steady state profile. The use of the other steady states as initial profiles leads to similar results as above and will not be shown here.

PACKED-BED REACTOR MODEL

It is evident from the results already quoted that the transient behavior of the internal phase of catalyst particles is quite complex and yields considerably more information than given by steady state profiles. In a transient operating packed-bed catalytic reactor this internal particle phenomenon is not the only transport process of importance; there is also the external field mixing and heat transfer in both axial and radial directions of the bed proper. Thus a mathematical description must couple these external field gradients through the film existing at the particle surface to the internal particle gradients plus chemical reaction.

Derivation of Model Equations

The mathematical model to be used to represent the external field, that is the interparticle field, is based upon the work of Deans and Lapidus (7). These authors represent the external field by a properly chosen two-dimensional array of CSTR's. Each axial row of CSTR's is taken to be one particle diameter in length with a total of N axial rows where $N = L/d_p$. The subscript i, $1 \leq i \leq N$, in all subsequent material here will be taken to indicate an axial row. The number of radial CSTR's within any axial row is denoted by the subscript j which takes on the values $j = \frac{1}{2}, 3/2, \cdots, M$ when i is an odd integer, and the values $j = 1, 2, \cdots, M$ when i is an even integer. M is defined by the relationship $2M = D_{Bed}/d_p$ and is an integer such that either the odd or even axial rows will have a half stage at the wall of the reactor.

Because of this half stage (or CSTR) arrangement, each axial row has stages which are offset or staggered from those in the rows immediately above and below itself. In any row i the j stage is fed heat and mass from the $i-1$ row and the $j - \frac{1}{2}$ and $j + \frac{1}{2}$ stages. The i,j stage in turn feeds two stages in the $i+1$ row. The volume of each individual stage consists, of course, of open voids from the external field and of solid particle. From the geometry of this arrangement the area of any stage is given by

$$A_j = \pi d_p^2 (2j - 1) \tag{19}$$

The open volume of any stage is given by

$$V_T = \epsilon \pi d_p^3 (2j - 1) \tag{20}$$

The volumetric flow rate is given by

$$Q_{i,j} = v \epsilon \pi d_p^2 (2j - 1) \tag{21}$$

and the number of spherical particles in the volume of each stage is

$$n = 6(1 - \epsilon) (2j - 1) \tag{22}$$

Based upon this arrangement it is possible to take mass and heat balances on the i,j stage. Thus a mass balance yields

$$Q_{i,j}[\phi_{i-1,j} - c_{i,j}] + (\text{transferred from particle}) = \epsilon V_T \frac{dc_{i,j}}{dt'} \tag{23}$$

where $\phi_{i-1,j}$ represents a weight-average feed to the i,j stage from the $i-1$ stages above it. But if the rate of transfer into a particle is given by a mass transfer type of equation, then

$$D_p \left.\frac{\partial c_{i,j}(S)}{\partial \rho}\right|_{\rho=1.0} = k_g R\,[c_{i,j} - c_{i,j}(S)] \tag{24}$$

Furthermore, the mass transferred from all the articles in the i, j stage is given by

$$\text{rate} = -\left.\frac{\partial c_{i,j}(S)}{\partial r}\right|_{r=R} \cdot (\text{total sphere area})$$
$$= -\left.\frac{\partial c_{i,j}(S)}{\partial \rho}\right|_{\rho=1.0} \cdot R\,6(1-\epsilon)(2j-1)\pi d_p^2 \tag{25}$$

Substituting Equations (20), (21), (24), and (25), into (23) one gets, after some algebraic manipulation

$$\phi_{i-1,j} - c_{i,j} - \frac{6k_g(1-\epsilon)}{v\epsilon}[c_{i,j} - c_{i,j}(S)] = \frac{d_p}{v}\frac{dc_{i,j}}{dt'} = \frac{dc_{i,j}}{dt} \tag{26}$$

The equivalent temperature balance follows in exactly the same manner to yield

$$\Psi_{i-1,j} - T_{i,j} - \frac{6h_f(1-\epsilon)}{v\rho_f c_f \epsilon}[T_{i,j} - T_{i,j}(S)] = \frac{dT_{i,j}}{dt} \tag{27}$$

The weighted inlet concentrations $\phi_{i-1,j}$ (and temperatures $\psi_{i-1,j}$) can be obtained from the corresponding $c_{i-1,j-1/2}$ and $c_{i-1,j+1/2}$ by rather straightforward algebraic equations; that is

$$\phi_{i-1,j} = \frac{(j-3/4)c_{i-1,j-1/2} + (j-1/4)c_{i-1,j+1/2}}{2j-1} \tag{28}$$

with special results at the center line and the fractional stage (on either odd or even rows) at the wall:

$$\phi_{i-1,1/2} = c_{i-1,1}$$
$$\phi_{i-1,M} = c_{i-1,M-1/2} \tag{29}$$

Equations (26) and (27) represent the transient mass and heat balance in the external field for adiabatic operation. For a nonadiabatic process the temperature balance must be changed at the wall of the fixed-bed reactor. Thus if the heat transfer resistances at the wall are lumped into a single overall heat transfer coefficient, the wall stage representation for Equation (27) becomes

$$\psi_{i-1,M} - T_{i,M} + \frac{h_w A_{w,i}}{Q_M \rho_f c_f}(T_{w,j} - T_{i,M}) - \frac{6h_f(1-\epsilon)}{v\rho_f c_f \epsilon}[T_{i,M} - T_{i,M}(S)] = \frac{dT_{i,M}}{dt} \tag{30}$$

But, as illustration, for a full wall stage the area and flow rates in the transfer term in Equation (30) are given by

$$A_{w,i} = 2\pi d_p^2 M \epsilon$$
$$Q_M = \epsilon v \pi d_p^2 (2M-1) \tag{31}$$

Analogous expressions exist for a fractional stage at the wall, and the balance becomes

$$\psi_{i-1,M} - T_{i,M} + N'_{ST}[T_{w,j} - T_{i,M}] - \frac{6h_f(1-\epsilon)}{v\rho_f c_f \epsilon}[T_{i,M} - T_{i,M}(S)] = \frac{dT_{i,M}}{dt} \tag{32}$$

where N'_{ST} = Stanton number for heat transfer

$$= \frac{h_w}{v\rho_f c_f}\left(\frac{2M}{2M-1}\right) \text{ for full stages}$$

$$= \frac{h_w}{v\rho_f c_f}\left(\frac{2M}{M-1/4}\right) \text{ for fractional stages}$$

Once the external field equations are defined, it is next necessary to specify the coupling equations across the film around the particles. These may be written (in dimensionless form) as

$$\left.\frac{\partial c_{i,j}(S)}{\partial \rho}\right|_{\rho=1.0} = \frac{k_g R}{D_p}[c_{i,j} - c_{i,j}(S)] \tag{33}$$

$$\left.\frac{\partial T_{i,j}(S)}{\partial \rho}\right|_{\rho=1.0} = \frac{h_f R}{k}[T_{i,j} - T_{i,j}(S)] \tag{34}$$

Finally the equations for transport of mass and heat plus chemical reaction inside the particles are added. But these are identical to Equations (12) and (13) and hold for each i,j stage. These may be written as

$$\alpha\frac{N_2}{4}\frac{\partial c_p}{\partial t} = \frac{\partial^2 c_p}{\partial \rho^2} + \frac{2}{\rho}\frac{\partial c_p}{\partial \rho} - \delta c_p e^{-\gamma\left[\frac{1}{T}-1\right]} \tag{35}$$

$$\frac{N_1}{4}\frac{\partial T_p}{\partial t} = \frac{\partial^2 T_p}{\partial \rho^2} + \frac{2}{\rho}\frac{\partial T_p}{\partial \rho} - \delta\beta c_p e^{-\gamma\left[\frac{1}{T}-1\right]} \tag{36}$$

The boundary and initial conditions necessary to complete the total system definition are

$$\left.\begin{aligned} c(i,j,0) &= c_1 \\ T(i,j,0) &= T_1 \end{aligned}\right\} \text{initial conditions in the external field} \tag{37}$$

$$\left.\begin{aligned} c_p(r,0) &= c_1(r) \\ T_p(r,0) &= T_1(r) \end{aligned}\right\} \text{initial conditions inside the particles} \tag{38}$$

$$\left.\begin{aligned} c(0,j,t) &= \bar{c}_1(t) \\ T(0,j,t) &= \bar{T}_1(t) \end{aligned}\right\} \text{feed to reactor} \tag{39}$$

$$T_w(i,M,t) = T_{\text{wall}} \quad \text{cooling fluid temperature}$$

$$\frac{\partial T_p}{\partial \rho} = \frac{\partial c_p}{\partial \rho} = 0,\ \rho = 0 \quad \left\{\begin{array}{l}\text{zero slope at} \\ \text{center of particles}\end{array}\right. \tag{40}$$

These equations and auxiliary conditions are sufficient to define the transient behavior of a packed-bed catalytic reactor subject to the assumptions made in the various derivations. As an example of the assumptions made, the fluid density is taken as constant in the external field equations. This restriction on the physical system and others may be removed (7), but only at the expense of an extensive addition in complexity and computing time.

Numerical Treatment of Model Equations

The procedure used for numerical integration of the transient fixed-bed reactor equations is based on the approximation of partial and ordinary differential equations by finite differences. Convergence of the resulting difference equations to a unique and real solution is not guaranteed for nonlinear equations of the form involved here. However the results of a variety of integrations seem to imply that no problems of this type exist in this particular case.

The replacement of derivatives by finite differences can take two paths, first a replacement to yield explicit types of difference equations or second a replacement to yield implicit types of difference equations (9). While the former approach yields a set of equations which are simple to solve, the time step which can be used is severely limited in order to maintain numerical stability of the solution. Since the implicit method does not involve this defect, implicit procedures are used whenever possible.

Particle Equations. As an illustration of the procedures

used the internal heat Equation (36) is taken:

$$\frac{N_1}{4}\frac{\partial T_p}{\partial t} = \frac{\partial^2 T_p}{\partial \rho^2} + \frac{2}{\rho}\frac{\partial T_p}{\partial \rho} - \delta\,\beta\,c_p\,e^{-\gamma\left[\frac{1}{T_p}-1\right]} \tag{36}$$

In defining a set of implicit difference equations the dependent variables are averaged over two time steps. With the subscript r used to indicate position in the radial direction in the particle, t indicate position in the time direction, and with the p subscript dropped for the moment, a suitable approximation of Equation (36) can be written as

$$\frac{N_1}{4}\left[\frac{T_{r,t+1}-T_{r,t}}{\Delta t}\right] = \frac{1}{2\Delta r^2}\left[(T_{r+1,t+1}-2T_{r,t+1}+T_{r-1,t+1}) + (T_{r+1,t}-2T_{r,t}+T_{r-1,t})\right] + \frac{1}{2\rho\Delta r}\left[(T_{r+1,t+1}-T_{r-1,t+1}) + (T_{r+1,t}-T_{r-1,t})\right] - \frac{\delta\beta}{2}e^{-\gamma\left[\frac{1}{T_{r,t}}-1\right]}(c_{r,t+1}+c_{r,t})$$

Collecting all T values at the $t+1$ time step on the left-hand side one can arrange this equation to the form

$$B_r{}^T T_{r+1,t+1} + A_r{}^T T_{r,t+1} + E_r{}^T T_{r-1,t+1} = D_r{}^T \tag{41}$$

where

$$B_r{}^T = -\left[\frac{1}{2\Delta r^2}+\frac{1}{2\rho\Delta r}\right]$$

$$A_r{}^T = \left[\frac{N_1}{4\Delta t}+\frac{1}{\Delta r^2}\right]$$

$$E_r{}^T = -\left[\frac{1}{2\Delta r^2}-\frac{1}{2\rho\Delta r}\right]$$

$$D_r{}^T = \left[\frac{1}{2\Delta r^2}+\frac{1}{2\rho\Delta r}\right]T_{r+1,t} + \left[\frac{N_1}{4\Delta t}-\frac{1}{\Delta r^2}\right]T_{r,t} + \left[\frac{1}{2\Delta r^2}-\frac{1}{2\rho\Delta r}\right]T_{r-1,t} - \frac{\delta\beta}{2}e^{-\gamma\left[\frac{1}{T_{r,t}}-1\right]}(c_{r,t+1}+c_{r,t}) \tag{42}$$

If one assumes that the index r increases from the center of the particle out to the surface and denotes the center by $r=1$ and the surface by $r=N+1$, Equation (41) holds for all $1 < r < N$. At the center of the pellet the boundary condition of Equation (40) modifies the equation so that

$$B_1{}^T T_{2,t+1} + A_1{}^T T_{1,t+1} = D_1{}^T \quad r = 1 \tag{43}$$

where

$$B_1{}^T = -\left[\frac{3}{2\Delta r^2}\right]$$

$$A_1{}^T = \left[\frac{N_1}{4\Delta t}+\frac{3}{\Delta r^2}\right]$$

$$D_1{}^T = \left[\frac{3}{\Delta r^2}\right]T_{2,t} + \left[\frac{N_1}{4\Delta t}-\frac{3}{\Delta r^2}\right]T_{1,t} - \frac{\delta\beta}{2}(c_{1,t+1}+c_{1,t})\exp-\left(\gamma\left[\frac{1}{T_{1,t}}-1\right]\right)$$

At $r=N$, the equation must also be modified to

$$A_N{}^T T_{N,t+1} + E_N{}^T T_{N-1,t+1} = D_N{}^T \quad r = N \tag{44}$$

where

$$E_N{}^T = -\left[\frac{1}{2\Delta r^2}-\frac{1}{2R\Delta r}\right]$$

$$A_N{}^T = \left[\frac{N_1}{4\Delta t}+\frac{1}{\Delta r^2}\right]$$

$$D_N{}^T = \left[\frac{1}{2\Delta r^2}+\frac{1}{2R\Delta r^2}\right]T_{N+1,t+1} + \left[\frac{1}{2\Delta r^2}+\frac{1}{2R\Delta r}\right]T_{N+1,t} + \left[\frac{N_1}{4\Delta t}-\frac{1}{\Delta r^2}\right]T_{N,t} + \left[\frac{1}{2\Delta r^2}-\frac{1}{2R\Delta r}\right]T_{N-1,t} - \frac{\delta\beta}{2}(c_{N,t+1}+c_{N,t})\exp\left(-\gamma\left[\frac{1}{T_{N,t}}-1\right]\right)$$

where $N+1$ refers to the surface temperature. Of course the mass balance, Equation (38), can be converted to an equivalent form in exactly the same way with the same meaning:

$$B_1{}^c c_{2,t+1} + A_1{}^c c^c{}_{1,t+1} = D_1{}^c \quad r = 1$$
$$B_r{}^c c_{r-1,t+1} + A_r{}^c c^c{}_{r,t+1} + E_r{}^c c_{r-1,t+1} = D_r{}^c \quad 1 < r < N$$
$$A_N{}^c c_{N,t+1} + E_N{}^c c_{N-1,t+1} = D_N{}^c \quad r = N \tag{45}$$

It will be noted that the average temperature is not used in the exponential expression for the rate constant. The use of the average temperature would make necessary an iterative type of solution in each cell for the exponential term and would measurably increase the computing time involved. It was felt that allowing the temperature in the exponential to lag one time step behind the rest of the solution would not seriously affect the accuracy of the results. The only apparent negative influence would be in the limitation of the size of the time step. Various time steps were used to decide how large this size could be before inaccuracies began to occur, and a conservative result was used in all subsequent calculations.

Equations (41), (43), (44), and (45), with (42) defining the coefficients, form a set of $2N$ simultaneous linear equations with the $2N$ values of the mass and temperatures at the $t+1$ step as unknowns. This assumes that all the values at that step are known; this follows directly from starting at $t=0$ with a given steady state profile and having as unknowns the values at $t = t+1$. Each set of equations has a tridiagonal coefficient matrix and can be put in the form, with the temperature balance for illustration

$$\mathbf{M}\,\mathbf{T} = \mathbf{D}^T$$

where

$$\mathbf{M} = \begin{bmatrix} A_1{}^T & B_1{}^T & & & & \\ E_2{}^T & A_2{}^T & B_2{}^T & & & \\ & \cdot & \cdot & \cdot & & \\ & & \cdot & \cdot & \cdot & \\ & & & \cdot & \cdot & B^T{}_{N-1} \\ & & & & E_N{}^T & A_N{}^T \end{bmatrix}; \quad \mathbf{T} = \begin{bmatrix} T_{1,t+1} \\ T_{2,t+1} \\ \cdot \\ \cdot \\ \cdot \\ T_{N,t+1} \end{bmatrix}; \quad \mathbf{D}^T = \begin{bmatrix} D_1{}^T \\ D_2{}^T \\ \cdot \\ \cdot \\ \cdot \\ D_N{}^T \end{bmatrix}$$

The method of solution is due to Thomas as detailed, for example by Lapidus (9), and is both fast and also efficient in the sense of minimizing round-off error propagation. Carberry and Wendel (6) have shown the application of this method of handling problems in diffusion, flow, and chemical reaction.

Film Equation Approximation. The equations for transport across the film surrounding each particle are (33) and (34). Using the heat balance

$$\left.\frac{\delta T_{i,j}(S)}{\delta \rho}\right|_{\rho=1.0} = \frac{h_f R}{k}\left[T_{i,j} - T_{i,j}(S)\right]$$

for illustration, one can obtain an implicit representation by averaging over the $t+1$ and t time steps. This yields

$$\frac{T_{i,j,t+1}(S) - T_{i,j,t}(S-1)}{\Delta r} = \frac{h_f R}{2k}\left\{\left[T_{i,j,t+1} - T_{i,j,t+1}(S)\right] + \left[T_{i,j,t} - T_{i,j,t}(S)\right]\right\}$$

Solving for the surface temperature at the $t+1$ time step one gets

$$\left[\frac{1}{\Delta r}+\frac{h_f R}{2k}\right]T_{i,j,t+1}(S)=\frac{1}{\Delta r}\left[T_{i,j,t}(S-1)\right]+\frac{h_f R}{2k}\left[T_{i,j,t+1}+T_{i,j,t}-T_{i,j,t}(S)\right] \quad (46)$$

The mass balance can be written in an analogous manner.

Several alternate representations were also formulated, but a testing of the stability properties of these other arrangements led to their being discarded. By contrast the above formulation proved quite stable over large variations of the size of the time step

External Field Approximations. When one uses the temperature balance, Equation (27), for the external field as an illustration

$$\psi_{i-1,j}-T_{i,j}-\frac{6h_f(1-\epsilon)}{v\rho_f c_f \epsilon}\left[T_{i,j}-T_{i,j}(S)\right]=\frac{dT_{i,j}}{dt}$$

an implicit formulation can be written as

$$\frac{\psi_{i-1,t+1}+\psi_{i-1,j,t}}{2}-\frac{T_{i,j,t+1}+T_{i,j,t}}{2}-\frac{6h_f(1-\epsilon)}{v\rho_f c_f \epsilon}\frac{1}{2}\{[T_{i,j,t+1}+T_{i,j,t}]-[T_{i,j,t+1}(S)+T_{i,j,t}(S)]\}=\frac{T_{i,j,t+1}-T_{i,j,t}}{\Delta t}$$

This equation can be solved for $T_{i,j,t+1}$, but the result still includes the surface temperature $T_{i,j,t+1}(S)$. This latter term can be eliminated by using Equation (46), and after the dimensionless group $N'_{STH}=\dfrac{6(1-\epsilon)h_f}{v\rho_f c_f \epsilon}$ is defined, there finally results

$$=\left\{\frac{1}{\Delta t}+\frac{1}{2}+\frac{N'_{STH}}{2}\left[1-\frac{1}{\frac{2k}{h_f R\Delta r}+1}\right]\right\}T_{i,j,t+1}$$

$$=\frac{1}{\Delta t}-\frac{1}{2}-\frac{N'_{STH}}{2}\left[1-\frac{1}{\frac{2k}{h_f R\Delta r}+1}\right]T_{i,j,t}+\frac{N'_{STH}}{2}\left[1-\frac{1}{\frac{2k}{h_f R\Delta r}+1}\right]T_{i,j,t}(S)+\frac{N'_{STH}}{2}\left[\frac{1}{1+\frac{h_f R\Delta r}{2k}}\right]T_{i,j,t}(S-1)+\frac{1}{2}(\psi_{i-1,j,t+1}+\psi_{i-1,j,t}) \quad (47)$$

In symbolic form Equation (47) can be represented as

$$T_{t+1}=f\left[T_t, T_t(S), T_t(S-1), \psi_{t+1}, \psi_t\right] \quad (48)$$

for the *i,j* stage. This specifies that the external field temperature at time step $t+1$ is calculated from the feed to the *i,j* stage, the surface temperature gradient, and the temperature of the external field at time step t. The mass balance can be written and solved in an analogous manner.

Overall Calculation Procedure. The overall calculation procedure is started by specifying an initial steady state distribution of mass and temperature throughout the entire reactor including the particles. The next step is to calculate the new mass and temperature profiles at the end of the first time step, after the column is subjected to a perturbation in mass and/or temperature in the feed stream to the reactor. Once these new values are all known, the calculation is repeated for the second time step and continued in the same manner until a new steady state is reached. Of primary interest here is the means of specifying the initial distribution and then the method for using this information to advance one time step.

To detail the latter procedure first, assume that the given distribution throughout the entire packed-bed reactor and the explicit perturbation in the feed stream are both known. When one uses Equation (28) and its temperature equivalent, the weighted average values $\phi_{0,j,t+1}$ and $\psi_{0,j,t+1}$ which serve as feed to the first row of CSTR's can be calculated. From Equation (47) and its mass equivalent the temperature and concentrations of the external field is each CSTR of the first row, $T_{1,j,t+1}$ and $c_{1,j,t+1}$, can be evaluated. From Equation (46) and its mass equivalent the particle surface temperatures and concentrations, $T_{1,j,t+1}(S)$ and $c_{1,j,t+1}(S)$, can be calculated. These latter values serve as a boundary condition for the calculation of the profiles inside the particles with Equations (41) and (45) used. This is continued across the entire first row of particles. Then the axial index is incremented and the second row of CSTR's evaluated, with the output of the row just calculated used as feed. In this way the entire bed distribution is determined for a single time step.

The only exception to this procedure occurs when a CSTR next to the wall is involved. Here the alternate Equation (22) is used to allow the cooling temperature of T_w to be included and to allow the use of full or fractional stages. As a brief side line the wall temperature was always taken as having a value of 0.5 or was taken as a linear interpolation between the feed temperature and 0.5. Both procedures correspond to easily realizable physical cooling systems.

The initial steady state distributions for the entire bed were obtained by first selecting a steady state distribution for one particle. By using this distribution for all the particles and any arbitrary set of external field values, the transient response to a constant set of feed conditions can be evaluated. The result of this transient calculation is a final steady state distribution within the particles and in the external field; these can be used subsequently as initial conditions for any further transient runs. All in all six different preliminary sets of calculations were carried out to generate such initial conditions. Two different feed temperatures were used with the three combinations of the different steady state profiles inside the catalyst particles discussed previously.

A SURFACE REACTION MODEL

Since the mathematical model proposed in this work extends most previous work in combining the internal particle problem with the external field, it is important to ascertain the effects of this added degree of complexity. Thus an alternate and simpler model, the surface reaction model, was set up to allow a subsequent computational comparison. In this new model all chemical reaction is assumed to take place on the external surface of the catalyst (no internal gradients). A one-dimensional (axial) form of this surface reaction model has been recently used by Liu and Amundson (*11*) to study stability problems in packed-bed reactors.

Obviously the external field equations for this surface reaction model are the same as previous, Equation (27) and its mass equivalent. A temperature balance which combines the surface reaction and the transport across the surface film yields, when converted to the previously used dimensionless variables and parameters, is

$$T_{i,j}-T_{i,j}(S)-\frac{2\delta\beta}{3N'_{Nu}}e^{-\gamma\left[\frac{1}{T_{i,j}(S)}-1\right]}c_{i,j}(S)=\frac{N_1}{6N'_{Nu}}\frac{\partial T_{i,j}(S)}{\partial t} \quad (49)$$

The equivalent mass balance is

$$c_{i,j} - c_{i,j}(S) - \frac{2\delta}{3N'_{Sh}} e^{-\gamma\left[\frac{1}{T_{i,j}(S)} - 1\right]} c_{i,j}(S) = \frac{N_2}{6N'_{Sh}} \alpha \frac{\partial c_{i,j}(S)}{\partial t} \quad (50)$$

The boundary and initial conditions required to complete the statement of this problem are identical to those defined previously except that instead of an initial profile inside the particles, only initial mass and temperature conditions on the surface are required.

The finite difference approximation used to represent this present model differ from the previous set in that only Equations (49) and (50) need be coupled with the external field, Equation (27) and its mass equivalent. An implicit representation for Equation (49) is given by

$$\frac{T_{i,j,t+1} + T_{i,j,t}}{2} - \frac{T_{i,j,t+1}(S) + T_{i,j,t}(S)}{2} - \frac{2\delta\beta}{3N'_{Nu}} e^{-\gamma\left[\frac{1}{T_{i,j,t}(S)} - 1\right]} \left[\frac{c_{i,j,t+1}(S) + c_{i,j,t}(S)}{2}\right] = \frac{N_1}{6N'_{Nu}} \left[\frac{T_{i,j,t+1}(S) - T_{i,j,t}(S)}{\Delta t}\right] \quad (51)$$

An equivalent mass formulation follows in exactly the same way.

Equation (51) and its mass equivalent may be solved for $T_{i,j,t+1}(S)$ and $c_{i,j,t+1}(S)$ and substituted into the external balances to yield equations in terms of $T_{i,j,t+1}$ and $c_{i,j,t+1}$. The complexity of these final equations prevents their being written here except in symbolic forms as follows:

$$T_{i,j,t+1} = f_1(T_{i,j,t};\ T_{i,j,t}(S);\ c_{i,j,t+1}(S);\ c_{i,j,t}(S);\ \psi_{i-1,j,t+1};\ \psi_{i-1,j,t}) \quad (52)$$

An analogous expression holds for $c_{i,j,t+1}$. The calculation procedure for Equation (52), the mass equation, coupled with the corresponding equations for surface temperature (51) and surface composition is equivalent to that discussed for the full internal particle system, the only difference being that a single temperature describes the particle response while previously a profile of temperatures was necessary.

PROGRAM DESCRIPTION

The model described above was simulated on an IBM-7090 computer. The equations as described in finite difference form were programed in Fortran II, and a completely self-contained program was designed to calculate first the steady state profiles in the particles and then to integrate the transient equations of the reactor subject to any perturbation in the feed desired.

The output of such a program could become voluminous in the extreme if some care had not been taken, and thus a variety of possible outputs were used. There is a subroutine available at the Princeton University computer center which allows curves to be displayed on a cathode-ray tube either for on-line monitoring or for permanent records by taking pictures on 35-mm. film. Also the output could be obtained in standard tabular form as printed on an off-line printer. In addition the availability of a subroutine to plot this tabular data with an off-line computer was used quite extensively.

In order to monitor what was occurring in the reactor, the cathode-ray tube was used frequently. This allowed the observance of either temperature or concentration profiles as they changed with time. This feature was also used in attempting to evaluate a stability criterion by watching the temperature curves change with time. The on-line printer was also available for printing of either slopes or profiles on-line if more exact results were required.

The timing of the program was constant for any one time step, while the computing time varied according to how many time steps were necessary and what size time step could be used while still maintaining accuracy. For the reactor used in most of the calculations, which contained forty-five cells, the time for the calculation of new set of profiles at time step $t+1$ required 25 sec. Each particle was divided into 150 internal radial increments for this computation time. A further descripton of the program appears in reference *12.*

RESULTS AND DISCUSSION

Details are presented here for a series of computer runs with the complete reactor model involving internal particle gradients. In addition a comparison is made between the full model, termed the *internal model,* and the surface reaction model. In the majority of cases a particular set of parameters were used, these being chosen on the basis of the occurrence of multiple steady state solutions inside the catalyst particles. In particular

$$\beta = \frac{\Delta H D_p c_o}{k T_o} = -0.6 \quad \text{(exothermic reaction)}$$

$$\gamma = E/R_1 T_o = 20.0$$

$$\delta = \frac{R^2 k_o}{D_p} = 0.25$$

lead to the three steady state distributions previously mentioned. In terms of the external field a suitable set of parameters corresponding to a significantly large reactor are, as given by Beek (3)

$N_1 = 705$	$N'_{Nu} = 55.3$
$N_2 = 1{,}225$	$N'_{STH} = 0.895$
$N'_{Sh} = 66.5$	$N'_{STM} = 0.605$
	$N'_{ST} = 2.0$

In addition, the bed length is taken as $L = 48$ and the bed diameter as $D_{bed} = 11$, in both cases based upon particle diameter. The initial and boundary conditions are given by

$T_{o,j} = 1.05$	, $t \geq 0$, all j
$c_{o,j} = 1.0$	, $t \geq 0$, all j
$T_{wall} = 0.5$	, $t \geq 0$, all i
$T_{i,j} = 1.0$	, $t < 0$, all i,j
$c_{i,j} = 1.0$	, $t < 0$, all i,j
$T_{i,j}(S) = T_1(\rho)$	, $t < 0$, all i,j,ρ
$c_{i,j}(S) = c_1(\rho)$	, $t < 0$, all i,j,ρ

$T_1(\rho)$ and $c_1(\rho)$ represent the steady state distribution within the particles corresponding to the middle reaction conditions discussed previously, and $T_{o,j} = 1.05$ indicates that the feed to the reactor is perturbed up from $T_{o,j} = 1.0$. For this set of parameters, the full system of equations was integrated as outlined previously.

Figure 3 shows the response of the axial row closest to the center line of the reactor to the feed temperature perturbation, and Figure 4 shows the external field steady state temperature profiles down the length of the reactor. As seen in Figure 3 the initial response is linear in nature and due entirely to the mixing phenomenon which occurs because of the particular design of the external model (7). After the small linear response passes through the bed, the nonlinear chemical reaction begins to make itself felt, and the temperature quickly begins to rise and reaches a

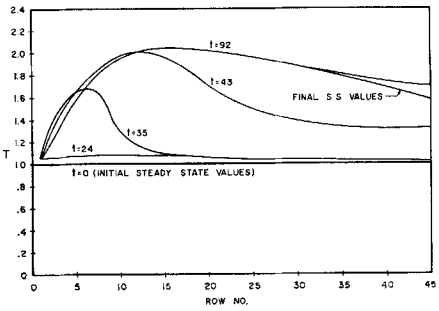

Fig. 3. Longitudinal temperature profiles for axial row closest to center line. Perturbation up in feed temperature to 1.05. $\beta = -0.6$, $\gamma = 20$, $\delta = 0.25$.

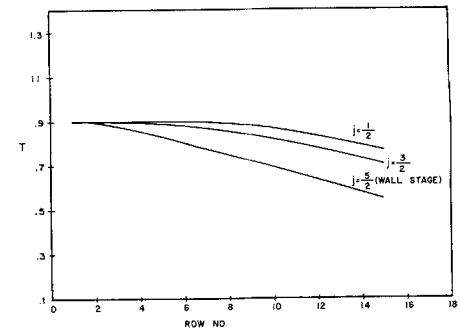

Fig. 5. Steady state longitudinal temperature profiles for various radial positions, small reactor for a feed of 0.9.

maximum or hot spot in the upper portion of the bed. This hot spot then passes down the reactor, rising as it progresses until it reaches a maximum temperature of approximately 2.05 at about one-third the way down the reactor. The coolant prevents this hot spot from continuing to rise and burn out the reactor. At the same time the catalyst particles have undergone changes in operating conditions and have moved to new equilibrium states. Those closest to the center line have the particles existing at the high reaction state (as defined previously), while those near the reactor wall, because of the low temperature of the external cooling fluid, exist at the low reaction state. Thus the individual particles are in differing steady states depending on their position in the reactor. This confirms the possibility of nonunique profiles due to differing initial conditions of the particles (*11*).

From Figure 4 it can be seen that the center-line stages, as expected, have the highest temperature as compared with stages closer to the reactor wall; in the same context (data not shown) concentration values show a similar (but in the reverse fashion) behavior. However, the magnitude of the concentration differences between radial positions is less than the corresponding temperature values.

A comment is in order at this point regarding the computing time involved to solve this problem. To obtain the results used in Figures 3 and 4 a prohibitive number of hours of IBM-7090 time was required. It was thus decided to make the reactor diameter equivalent to 5 d_p's and the reactor length equivalent to 15 d_p's. These changes represent a decrease in the total number of stages by a factor of about 7; when this change is combined with information obtained on the feasible time step size for integration, the calculation of the complete transient response of this new reactor could be evaluated in less than 3 hr. This was considered satisfactory to allow further calculations to be carried out.

The use of a bed length equivalent to 15 d_p's represents, of course, a very short bed. However, the initial value nature of the external field model means that increasing the bed length to say thirty or fifty d_p's will not change the concentration and temperature profiles in the first 15 d_p's. Thus the present length shows the major effects to be observed in any bed length.

STABILITY OF A PACKED-BED REACTOR

It is of both theoretical and practical importance to be able to specify whether a packed-bed reactor is stable or unstable to feed perturbations. A stable reactor is here defined as one which, when perturbed, moves away from an initial steady state but then returns to the original steady state when the perturbation is removed. Even for a simple reactor such as a CSTR the specification of stability is not a trivial matter. The use of Liapunov's method has resulted in some interesting and important results (*10, 16*). The problem in the packed-bed reactor case is complicated not only by the nonlinearity of the equations involved but also by the possible existence of the multiple steady state distributions. It should also be emphasized that physical stability must be considered along with mathematical stability. In other words, it is quite possible that in moving from the initial condition to the final condition very high temperatures may be reached in certain portions of the bed. These temperatures may result in physical instabilities, in the sense that the reactor burns up, which a mathematical analysis will in no way recognize.

In the present system the results of many transient calculations show that the size of the perturbation is important and that some portions of the bed may return to their original conditions while other portions pass on to new steady states. On this basis the establishment of an analytical criteria which covers these complicated phenomena would seem to be a most difficult, if not impossible, undertaking. As a consequence it might be suggested that one actually surveys the results of simulating the transient behavior of a bed to see if some simple qualitative parameter can be selected to serve as a suitable stability indicator. As an illustration the temperature-time slope in the reactor might be used as a measure. An extremely

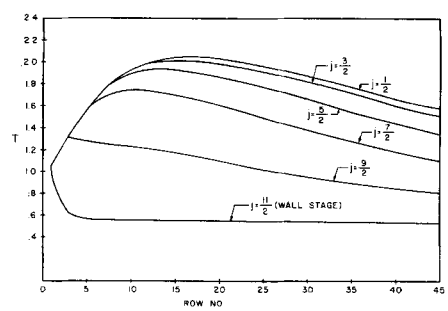

Fig. 4. Steady state longitudinal temperature profiles at various radial positions.

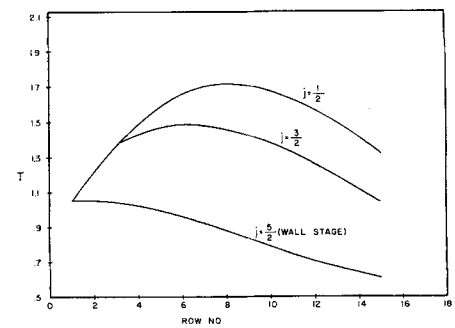

Fig. 6. Steady state longitudinal temperature profiles for a feed temperature of 1.05.

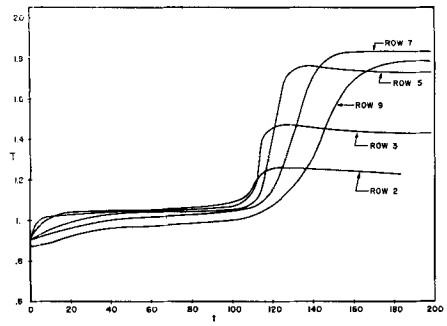

Fig. 7. Temperature response of several axial cells to a feed temperature of 1.05.

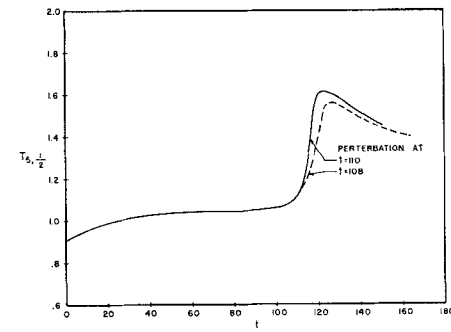

Fig. 9. Temperature response of axial cell in Row 5 to two different feed perturbations.

large slope would indicate the possibility of a run-away condition, whereas a moderate slope would indicate a stable type of operation. Where this slope should be evaluated and what is to be considered a large value are, however, serious questions. It was decided in the present work to use the external field temperatures, since these normally can be experimentally measured, and to use the centerline position in the reactor, since the maximum temperature rise occurs at this point.

In all future calculations mentioned in this paper, the initial profiles are the same. These steady states were obtained by calculating a complete transient response, of the smaller bed detailed above, to a feed temperature of 0.9. The initial particle profiles of this calculation correspond to the low reaction state. The resulting temperature profiles shown as a function of the row number are given in Figure 5.

In order to determine the maximum value of temperatures and slopes expected, a complete transient response of the packed bed reactor to a feed of 1.05 was calculated using as initial profiles the steady state values calculated with a feed of 0.9. The results of this transient analysis qualitatively follow the lines previously discussed with a long period in which most of the transfer occurs by mixing, with the source being the higher temperature of the feed stream. Then, because of the particles moving from the state of low reaction to high, the temperature begins to rise very rapidly and creates a hot spot in the reactor. This hot spot is then passed by the mixing mechanism down the reactor until the coolant temperature modifies its effect. The final external field temperature profiles are shown in Figure 6. The transient response of the temperature in the axial cell on rows 2, 3, 5, 7, and 9 is shown in Figure 7.

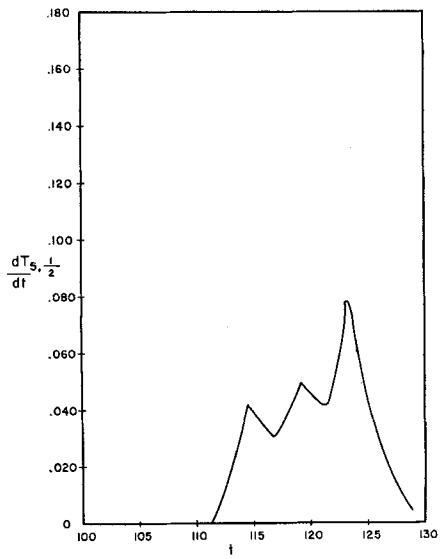

Fig. 8. Temperature-time slope of axial cell in fifth row as a function of time, feed temperature of 1.05. $\beta = -0.6$, $\gamma = 20$, $\delta = 0.25$.

As the parameter selected to try to characterize the stability is the temperature-time slope at several points down the column in the cells next to the center line, data were taken on this particular run to decide how this slope changes with time and whether any conclusions could be drawn from such data. A typical curve is shown in Figure 8, where the temperature-time slope of the axial cell on the fifth reactor row is plotted vs. time. As can be seen, there are not one but three maxima in the curve, corresponding to the passing of hot temperature waves down the reactor. Actually the curves are discrete rather than continuous, and more maxima could possibly have occurred. These first two maxima correspond to the rows above the fifth passing from the low temperature steady state to a high temperature steady state, with the temperature rise thus created being passed through the reactor by the mixing mechanism of the external field model. The last maximum is caused by the particles on this particular row passing from the low reaction state to the high, with the corresponding rapid increase in temperature.

The question to be investigated next deals with the effect of the duration of a perturbation in temperature in the feed stream; that is what happens to the reactor, which initially is at a steady state corresponding to a feed temperature of 0.9, when the feed temperature is perturbed up to 1.05, held for a period of time, and then dropped back to 0.9. Figure 9 illustrates this point with the temperature in the axial cell of row 5 plotted vs. time for a perturbation duration of $t = 108$ and $t = 110$. These two times were chosen specifically because they correspond to a very large value of the temperature-time slope in the axial cell of row 2. It can be seen that while there are differences in the temperature profiles, the final result is to approach the same steady state condition. This steady state point is quite different than the original starting steady state. From these data and others not shown the conclusion can be drawn that some other parameter other than the temperature time should be chosen to characterize stability. As seen in Figure 9, this parameter in row 5 serves only as an indication of what has already occurred. Any corrective action based on this parameter would not have any effect on the final operating state but only on the method of getting there, that is by passing through a smaller temperature hot spot which could possibly keep physical instabilities from occurring in the reactor itself.

The data illustrated show the response of the axial cells to the feed temperature change and suggest strongly that the stability of the reactor is not merely a function of what occurs in the external field but also a function of the reaction and transport parameter inside the particles themselves. If there was adequate space in this paper, profiles of each individual particle's response could be shown. In

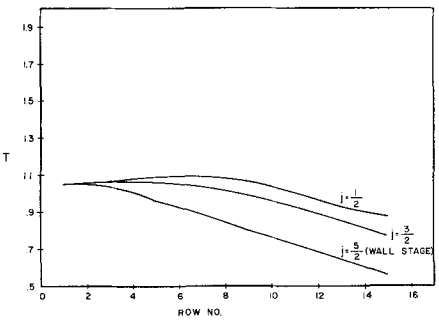

Fig. 10. Steady state longitudinal temperature profiles for various axial rows, surface reaction model, feed temperature of 1.05.

this case, the moving of the entire reactor from one steady state to another is accompanied, or perhaps even preceded, by the particles closer to the center line moving to a new reaction state. In order to ascertain whether or not the particular reaction parameters which give the multiple equilibrium states inside the particle will also be the only parameters which will give the multiple steady states in the entire reactor, a new value of β was chosen and various transient responses were calculated with all the other parameters identical. As can be seen from the definition for β in Equation (6), it is directly proportional to the heat of reaction, and thus a decrease in the value of β corresponds to a proportional decrease in the heat of reaction. A value of $\beta = -0.3$ was chosen because for this value of β and the values of γ and δ given previously, there exists a single steady state in the particles.

The first step in the procedure was to calculate a set of steady state profiles corresponding to a feed temperature of 0.9. This was carried out in the same manner as described above, except in this case there existed a single steady state profile inside the particles as determined from the steady state equation for the particle. With the steady state profiles calculated in this manner used as initial values for subsequent stability runs, several different feed temperature perturbations were used in an attempt to force the reactor to move from one steady state operating point to another as occurred above. The first perturbation was to a feed temperature of 1.05, and the only response from the reactor was to adjust the temperature profiles down the column to a slightly higher value corresponding to the higher feed temperature. The adjustment was caused solely by the mixing mechanism of the model, and the particles did not move from one operating state to another. Also the temperature-time slope at any place in the column never exceeded 5×10^{-3} in arbitrary units. This corresponds to a value about an order of magnitude less than that which occurred in the case where $\beta = -0.6$.

To further demonstrate whether or not the particles are the factors which contribute to the instability or stability a larger perturbation was used. In this case the feed temperature was perturbed to 1.2. Again the response was identical to that described above for the smaller perturbation. The reactor merely moved slightly to compensate for the higher feed temperature, and then when the perturbation was removed, the reactor returned to the original steady state. Thus it seems that the instability of the entire reactor is characterized by the existence of instabilities inside the particles. However, it is theoretically possible, for a particular set of parameters where the particle multiple solutions do not exist but a small change in the value of one of the parameter causes multiple solutions, that the coupling of the individual particles together in this particular model could make the entire reactor unstable while the individual particles remain stable. This point was not covered in the present work as it would have involved a much more extensive parameter investigation than is justified until a better or faster computer system is available.

The fact that it has been shown that for a particular set of parameters which lead to multiple solutions in the particles also lead to instabilities in the reactor bed itself, while conversely a set of parameters which give a unique solution in the particle and a bed which is stable does not preclude areas of parameters where this generalization is not true. However, the results lend themselves to the conclusion that a criterion of the form suggested by Weisz and Hicks (*17*) for the internal particle system may be adequate to characterize an entire packed-bed reactor.

COMPARISON OF SURFACE REACTION AND INTERNAL MODELS

A model where the reaction takes place solely on the external particle surface with no internal gradients was developed in a previous section. This model is much simpler than the internal model, and a complete transient response could be simulated in roughly 1/100 of the time necessary for the more complete model.

First, a comparison is to be carried out of the steady state solutions for these two different models to determine if this can yield a reason for selecting the more complex model. In Figures 6 and 10 the steady state temperature profiles of the internal and surface reaction models, respectively, are shown. The same feed temperature (1.05) was used in both cases, and the parameters for reaction and transport are identical. For this particular feed temperature there appears to be a difference in the steady state profiles with the difference in the maximum temperature being about 0.7 for the two columns closest to the center line but good agreement at the wall stages. By contrast, when a feed temperature of 1.1 is used, the difference in the steady state profiles is almost nonexistent. The curves start out with the same slope down the column with the only difference occurring at about row 8 where the maximum temperature of the surface reaction model is approximately 10% greater than the corresponding maxima of the internal model. If a design were based on one model vs. the other, the design which uses the surface reaction model as a basis would be more conservative but not by a large factor. Therefore on the evidence offered by the steady state results, the surface reaction model is to be preferred because of the approximation to the more complicated model and the much smaller computing time necessary for a complete simulation.

As has been mentioned before, the steady state analysis usually does not tell the entire story, and in this case this is once again proven true. The approach to steady state from a perturbation in feed temperature is very different for the two models. As described above, the internal model response shows an initial long period of heat transfer by the mixing mechanism; at about a dimensionless time of 120 the particles in the cell begin passing from the low reaction state to the high (using the axial cell on row 5 as a criterion). The slope of the temperature change with time shows the characteristic multiple maxima as before; finally at a time of around 160 the cell approaches a new steady state value. By contrast, in the surface reaction system the response is quite different from that of the internal reaction model. The initial temperature rise occurs quite quickly and then starts to level off. Then there is a sharp almost spike temperature rise, almost to the maximum value which the temperature reaches in this cell. After this a long period of time occurs with no further temperature increase. Then at a dimensionless time of around 420 the temperature again takes a sharp rise to the final steady state value. Other results using different parameters indicate that this behavior is typical and that

the differences between the two models are significant.

The conclusion which can be drawn from these results is that the transient response is very different for the two models and that any simulation scheme based solely on a surface reaction model will give misleading results. This also follows from the previous discussion in which it was seen that the internal system seemed to characterize the overall bed behavior. This is very important in that it implies that for a reaction which has a significant heat of reaction occurring in a system with porous pellets, the entire model must be considered to be able to draw realistic conclusions regarding the approach to steady state.

ACKNOWLEDGMENT

The authors wish to thank the International Business Machine Corporation and the National Science Foundation (Grant No. GP-506) for financial support in the form of research grants. In addition, the first author was pleased to hold a National Science Foundation Fellowship during a major period of this investigation. This work made use of computer facilities supported in part by National Science Foundation Grant NSF-GP579.

NOTATION

Independent Variables

ρ = dimensionless sphere radius (based on $d_p/2$)
t = dimensionless time length (based on d_p/v)
x = dimensionless axial length (based on d_p)

Dependent Variables

c = dimensionless concentration [based on $c_p(R)$]
T = dimensionless temperature [based on $T_p(R)$]
T_w = dimensionless wall temperature

Dynamic Moduli

$N_1 = \dfrac{d_p v\, \rho_s\, c_s}{k}$

$N_2 = d_p\, v/D_p$

N'_{Nu} = modified Nussult number $h_f\, d_p/k$
N'_{Sh} = modified Sherwood number $k_g\, d_p/D_p$
N'_{St} = modified Stanton number

$$(h_w/v\rho_f c_f)\left(\frac{2M}{2M-1}\right) \text{ full stage}$$

$$(h_w/\rho_f c_f)\left(\frac{2M}{M-1/4}\right) \text{ fractional stage}$$

$N'_{STN} = \dfrac{6h_f(1-\epsilon)}{v\rho_f c_f \epsilon}$

$N'_{STM} = \dfrac{6k_g(1-\epsilon)}{v\epsilon}$

$N_R = -a\, c'\, e^{-E/R_1 T'}$

a = frequency factor in Arrhenius expression
A = cross-section area of a stage
A_w = wall area of a stage
c_f = molar heat capacity of fluid
c_s = heat capacity of particles
c' = real particle concentration
D_{bed} = tube diameter
D_f = diffusivity of external fluid
D_p = diffusivity of particle fluid
d_p = diameter of catalyst particles
E = activation energy
ΔH = heat of reaction
h_f = heat transfer coefficient in fluid
h_w = heat transfer coefficient at the wall
k = thermal conductivity of porous solid
k' = reaction rate coefficient
k_g = mass transfer coefficient
k_o = reaction rate coeffcient evaluated at $[T_p(R)]$
L = length of bed
M = dimensionless tube radius and number of stages in a radial row
N = number of axial rows
n = number of particles in each cell defined by Equation (22)
Q = total volumetric flow rate to a given stage
R = radius of particles
R_1 = gas constant
Δr = radial increment in particle
S = surface value
t' = real time
Δt = dimensionless finite time increment
T' = real particle temperature
V_T = open volume of a stage
v = interstitial velocity of fluid

Greek Letters

α = void fraction of particle
β = dimensionless heat of reaction parameter defined by (6)
γ = dimensionless activation energy defined by (6)
δ = dimensionless diffusion parameter defined by (6)
ϵ = void fraction of the packed bed
μ = viscosity of fluid
ρ_s = density of catalyst packing
ρ_f = molar density of fluid
ϕ = dimensionless average feed concentration
ψ = dimensionless average feed temperature

Subscripts

f = fluid field
i = axial flow of stages or axial position in finite difference mesh
j = radial position of stage in a given row
p = dependent variables in particle field
r = radial position in particle finite mesh
s = particle field
t = time in finite time mesh
w = variable at wall position

LITERATURE CITED

1. Aris, Rutherford, and N. R. Amundson, *Chem. Eng. Sci.*, **7**, 121 (1958).
2. Barkelew, C., *Chem. Eng. Progr. Symposium Ser. No. 25*, **55**, 37 (1959).
3. Beek, John, *A.I.Ch.E. Journal*, **7**, 337 (1961).
4. ———, "Advances in Chemical Engineering," Vol. 3, Academic Press, New York (1962).
5. Carberry, J. J., *A.I.Ch.E. Journal*, **7**, 350 (1961).
6. ———, and M. M. Wendel, *ibid.*, **9**, 129 (1963).
7. Deans, Harry, and Leon Lapidus, *ibid.*, **6**, 656 (1960).
8. Lapidus, Leon, and Saul Shapiro, Paper presented at A.I.Ch.E. Meeting, Cleveland (May, 1961).
9. ———, "Digital Computation for Chemical Engineers," McGraw-Hill, New York (1962).
10. Leathrum, James, E. F. Johnson, and Leon Lapidus, *A.I.Ch.E. Journal*, **9**, 6 (November, 1963).
11. Liu, S., and N. R. Amundson, *Ind. Eng. Chem. Fundamentals*, **2**, 183 (1963).
12. McGuire, M. L., Ph.D. dissertation, Princeton University, Princeton, New Jersey (1964).
13. Prater, C. D., *Chem. Eng. Sci.*, **8**, 284 (1958).
14. Schillson, R. E., and N. R. Amundson, *Chem. Eng. Sci.*, **13**, 226 (1961).
15. van Heerden, C., *Ind. Eng. Chem.*, **45**, 1242 (1953).
16. Warden, R. B., R. Aris, and N. R. Amundson, *Chem. Eng. Sci.*, **19**, 149, 173 (1964).
17. Weisz, D. B., and J. S. Hicks, *ibid.*, **17**, 265 (1962).
18. Wilhelm, R. H., *Pure and Applied Chemistry*, **5**, 403 (1962).

Manuscript received December 30, 1963; revision received June 29, 1964; paper accepted July 10, 1964.